Electronic Supplementary Material (ESI) for Journal of Materials Chemistry A.

Two Viologen-Functionalized Pyrazolide-Based Metal-Organic Frameworks for Efficient CO_2 Photoreduction Reaction

Yuxin Xie [a, b], Chenghao Yao[a, b], Lei Li [a, b]*, Zhan Lin [a, b]*

[a] *Jieyang Branch of Chemistry and Chemical Engineering Guangdong Laboratory, Jieyang 515200, China*

[b] *Guangdong Provincial Key Laboratory of Plant Resources Biorefinery, School of Chemical Engineering and Light Industry, Guangdong University of Technology, Guangzhou 510006, China*

1. Synthesis of 1,1‘-bis(2,4-dinitrophenyl)-[4,4’-bipyridine]-1,1‘-diium

As shown in Scheme S1, the 1,1‘-bis(2,4-dinitrophenyl)-[4,4’-bipyridine]-1,1‘-diium dichloride (denoted as L_{11}) was synthesized according to the previous report literature procedure with a little modify. Typically, 4,4’-bipyridine (3.6 g, 23 mmol) and 1-chloro-2,4-dinitrobenzene (16.5 g, 81 mmol) were dissolved in 70 mL of CH_3CN. The reaction mixture was stirred under N_2 atmosphere at 85 ℃ for 72 h. The final suspension was filtered and subsequently washed with CH_3CN (3×20 mL), faint yellow solid is obtained. Then the resulting faint yellow powder was dried under vacuum at 80 ℃ for 12 h to give the product L_{11}. L_{11}: ^1H NMR (400 MHz, D_2O, Figure S1): δ 9.43~9.46 (CH, 4H), 9.37 (CH, 2H), 8.87~8.93 (CH, 6H) and 8.25~8.28 ppm (CH, 2H). Elemental analysis: For $C_{22}H_{14}O_8N_6Cl_2$ (M.W. 561.29): C, 47.08; H, 2.51; N, 14.97 wt%.

2. Synthesis of 1,1'-di(1H-pyrazol-4-yl)-[4,4'-bipyridine]-1,1'-diium dichloride

As shown in Scheme S1, to 2 g (3.56 mmol) of 1,1‘-bis(2,4-dinitrophenyl)-

[4,4'-bipyridine]-1,1'-diium dichloride and 0.62 g (7.46 mmol) of 4-Amino-1H-pyrazole in 50 mL of ethanol. The mixture is stirred together at 80 °C for 48 h, then cooled to room temperature. The atrovirens product was collected by centrifugation and washing several times with ethanol, followed by vacuum drying at 60 °C for 12 h. The ligand was obtained as an atrovirens powder. Ligand: ^1H NMR (400 MHz, D_2O, Figure S2): δ 13.67~13.69 (NH, 2H), δ 9.27~9.32 (CH, 4H), 8.63-8.67 (CH, 4H) and 8.33~8.37 ppm (CH, 4H). For $C_{16}H_{14}N_6Cl_2$ (M.W. 361.23, Figure S3): C, 53.15; H, 3.88; N, 23.25 wt%.

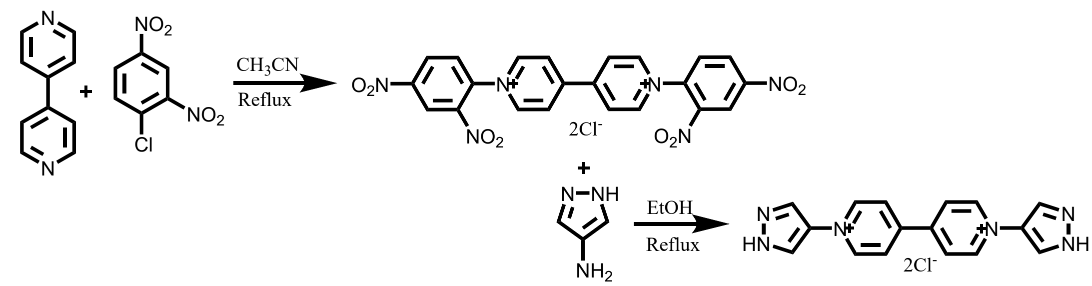

Scheme 1. Schematic illustration of the synthesis process of ligand.

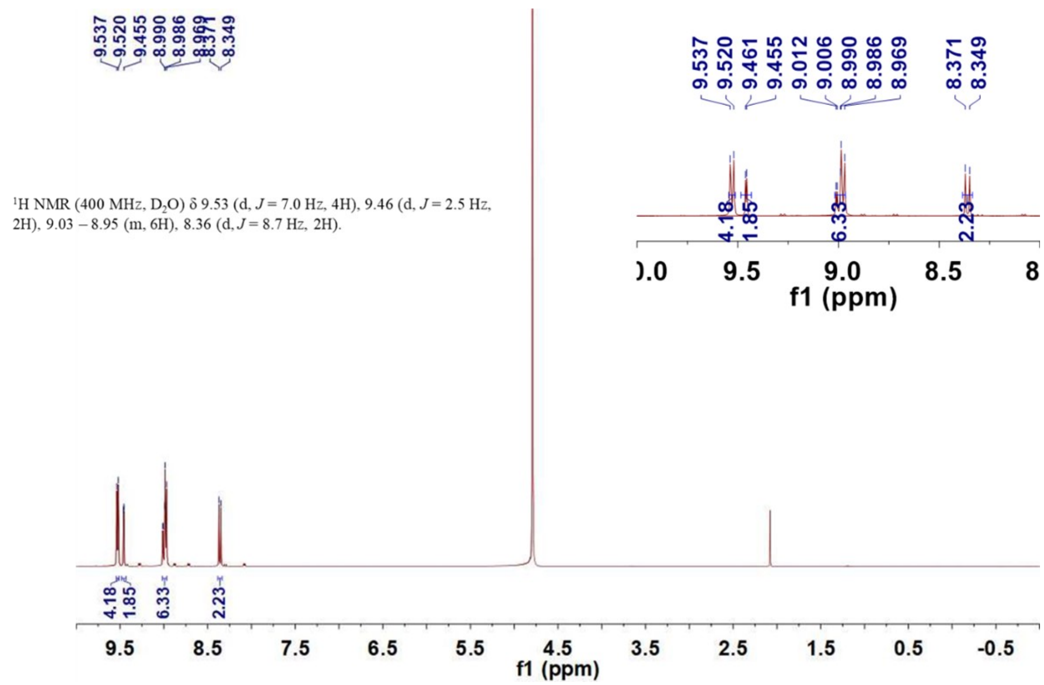

Figure S1. The ^1H NMR (400 MHz, D_2O) of L_{11} (1,1'-bis(2,4-dinitrophenyl)-[4,4'-bipyridine]-1,1'-diium dichloride).

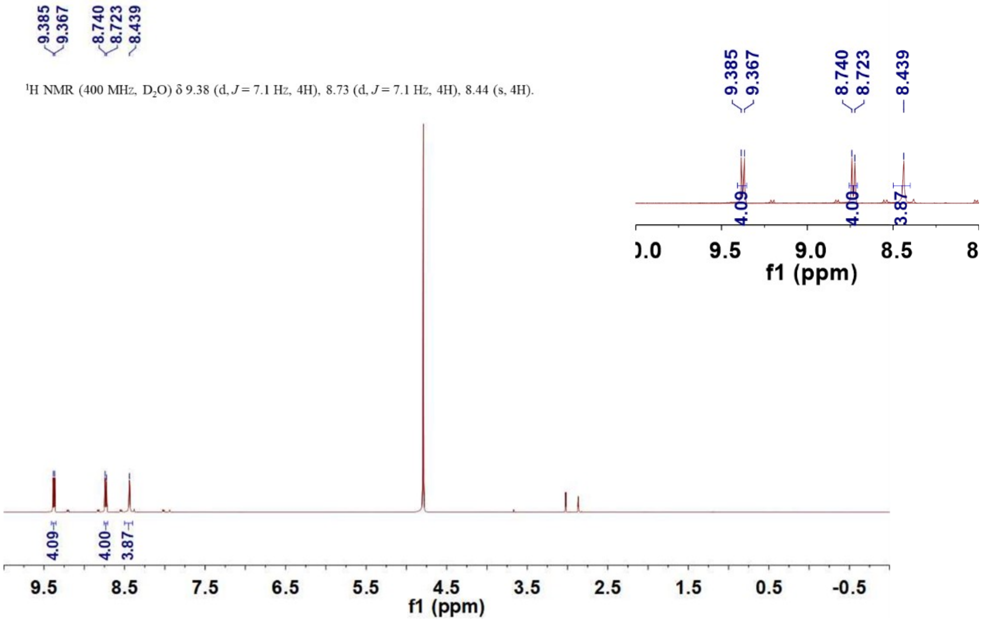

Figure S2. The ${}^{1}H$ NMR (400 MHz, D_2O) of ligand(1,1'-di(1H-pyrazol-4-yl)-[4,4'-bipyridine]-1,1'-diium dichloride).

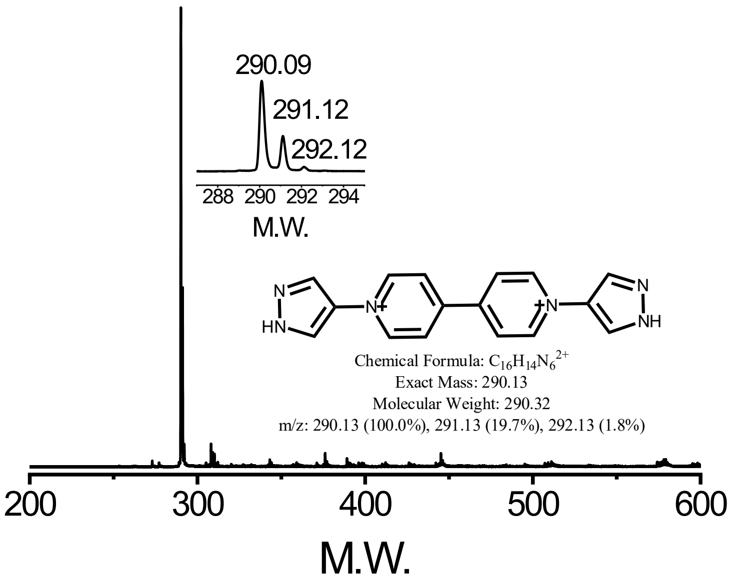

Figure S3. The MS (mass spectrometry) of ligand.

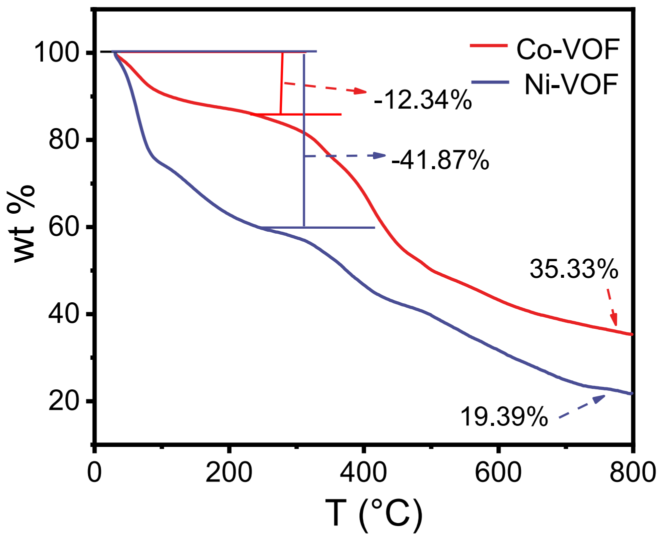

Figure S4. TG curves in N_2.

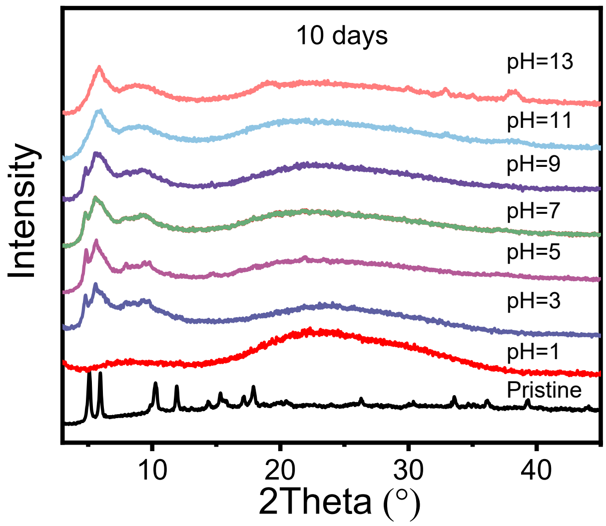

Figure S5. Powder X-ray diffraction (PXRD) patterns of Ni-VOF under different conditions.

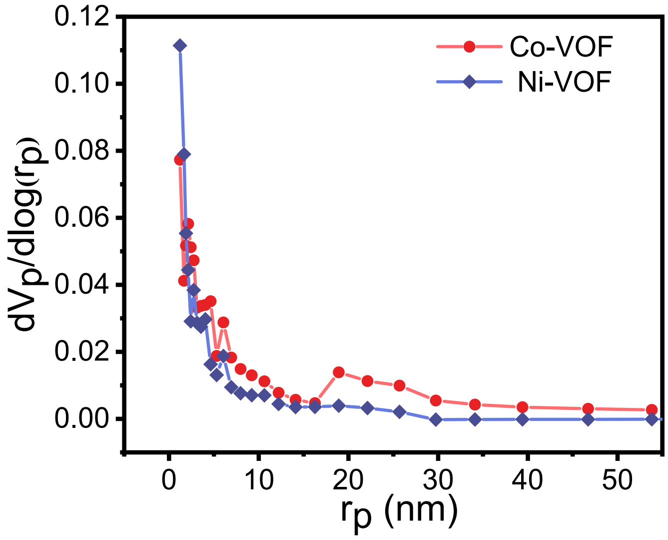

Figure S6. The pore distribution of Ni-VOF and Co-VOF.

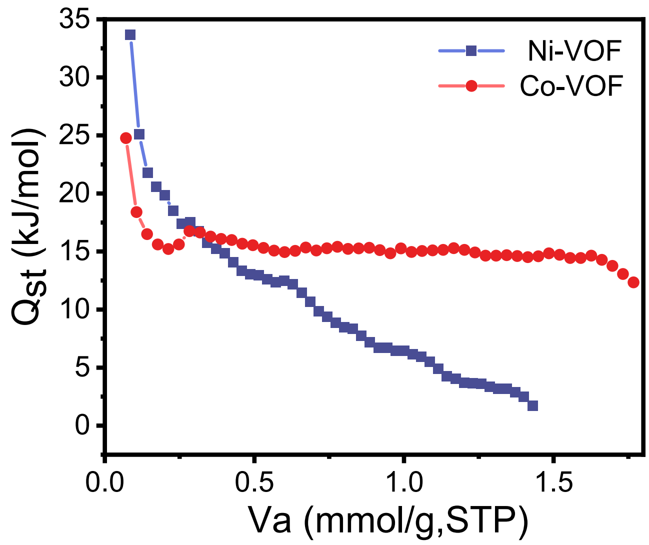

Figure S7. Isosteric heat of adsorption (Q_{st}) profiles of the samples for CO_2.

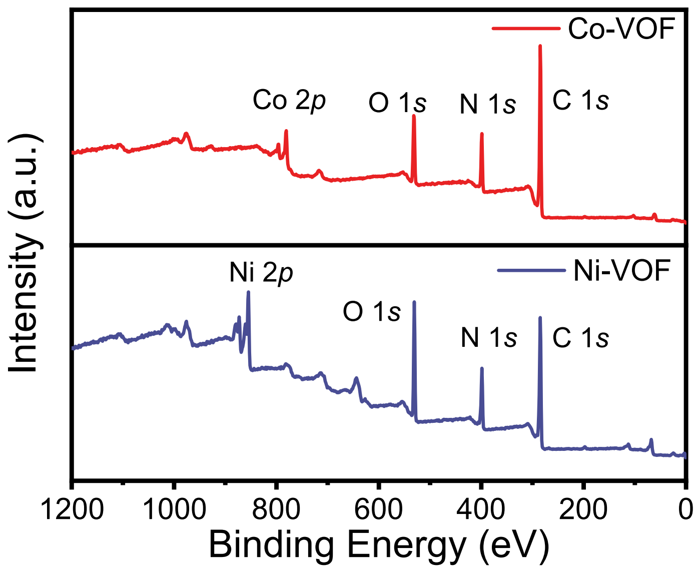

Figure S8. XPS survey spectrum of Co-VOF and Ni-VOF.

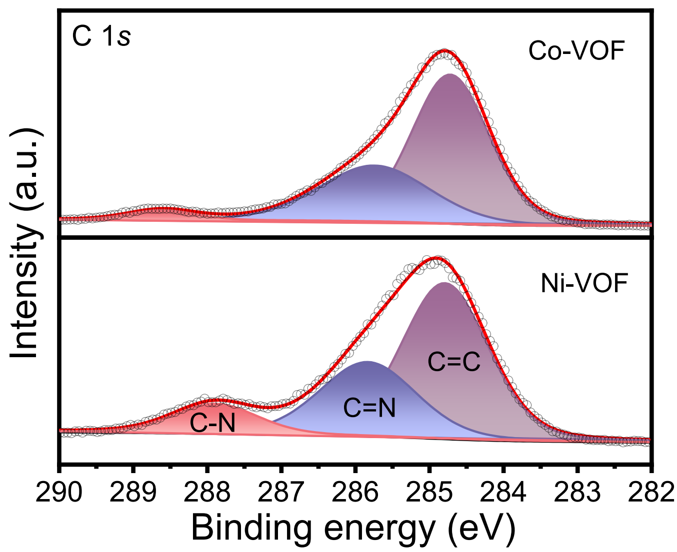

Figure S9. C 1*s* of Co-VOF and Ni-VOF.

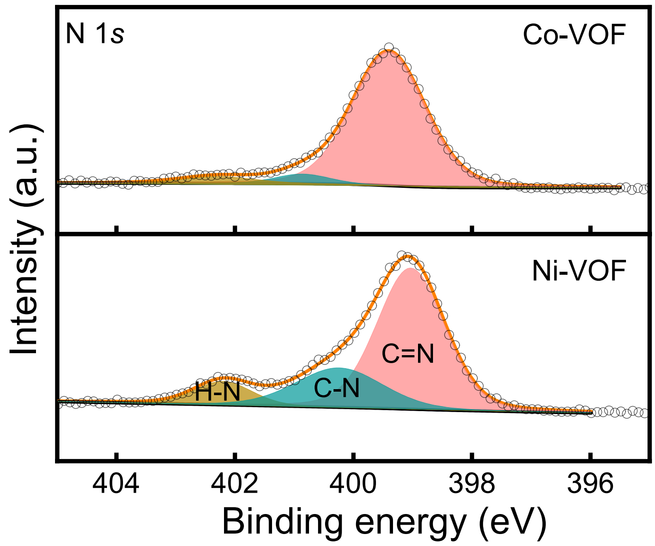

Figure S10. N 1*s* of Co-VOF and Ni-VOF.

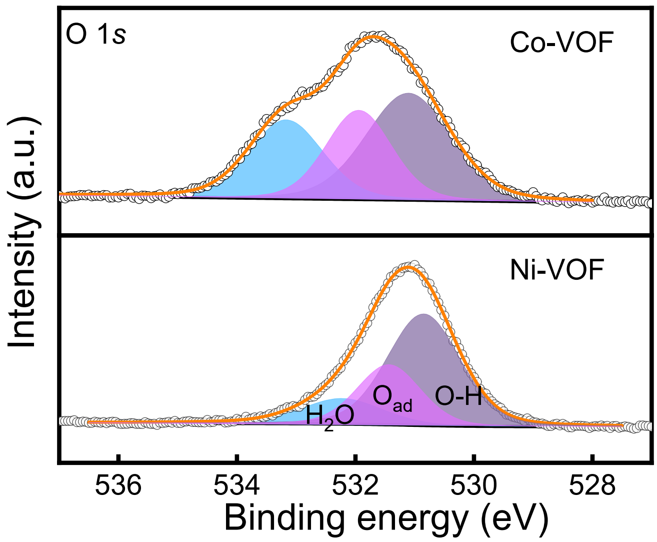

Figure S11. O 1*s* of Co-VOF and Ni-VOF.

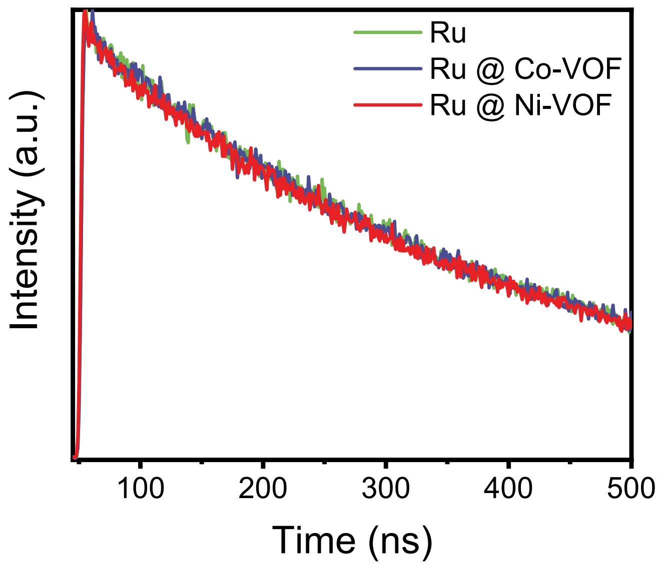

Figure S12. TCSPC experiment of Ni-VOF and Co-VOF. The samples were excited with a λ_{ex} = 450 nm laser and emission was observed at λ_{em} = 625 nm.

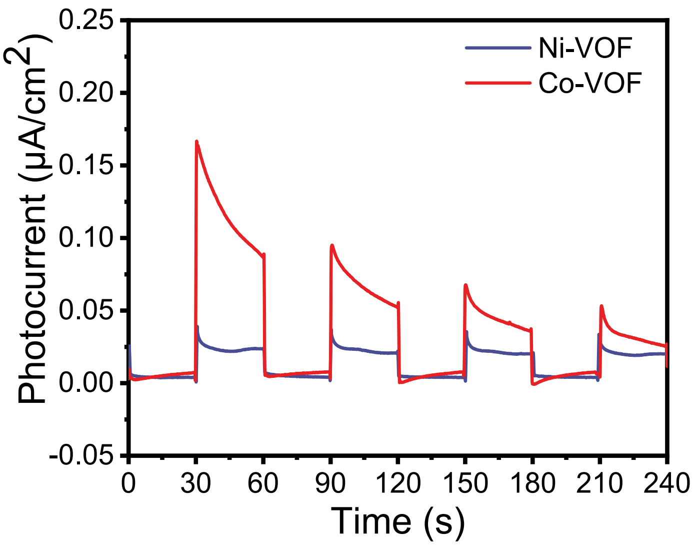

Figure S13. Transient photocurrent curves of Ni-VOF and Co-VOF.

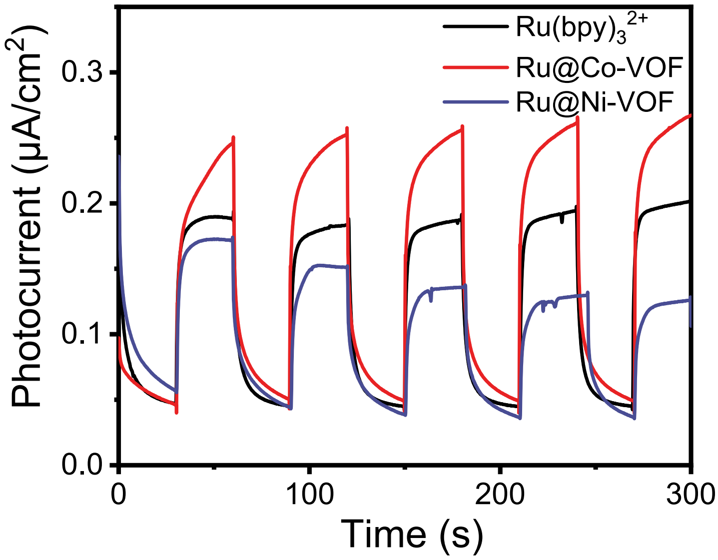

Figure S14. Transient photocurrent curves $Ru(bpy)_3^{2+}$, Ru@Ni-VOF and Ru@Co-VOF.

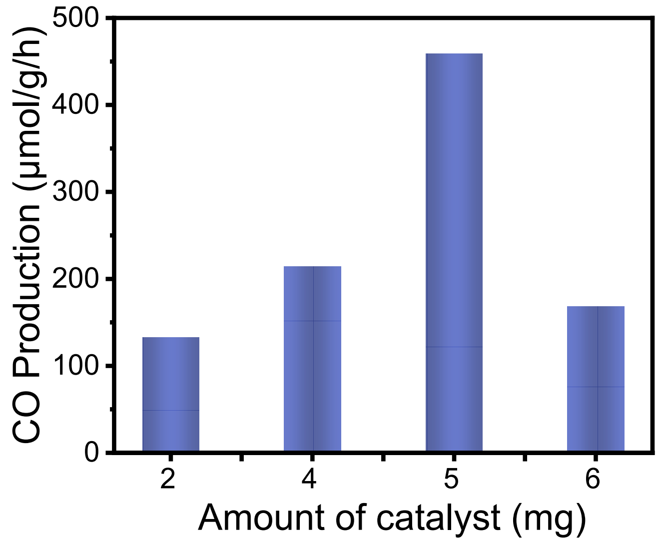

Figure S15. Effect of Co-VOF dosage on the formation rate of CO.

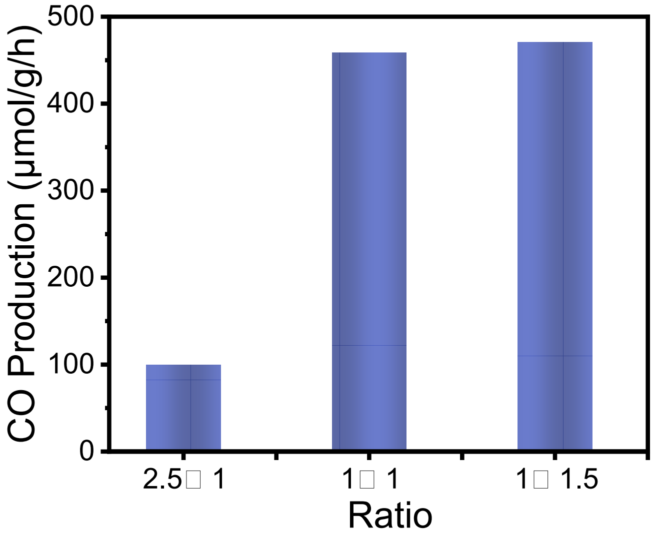

Figure S16. Effect of Co-VOF and Ru dosage ratio on the formation rate of CO.

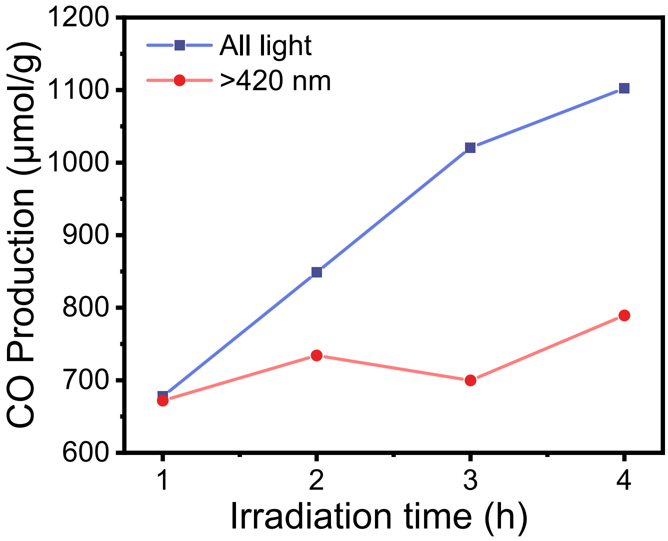

Figure S17. CO_2 photoreduction performance under various reaction conditions.

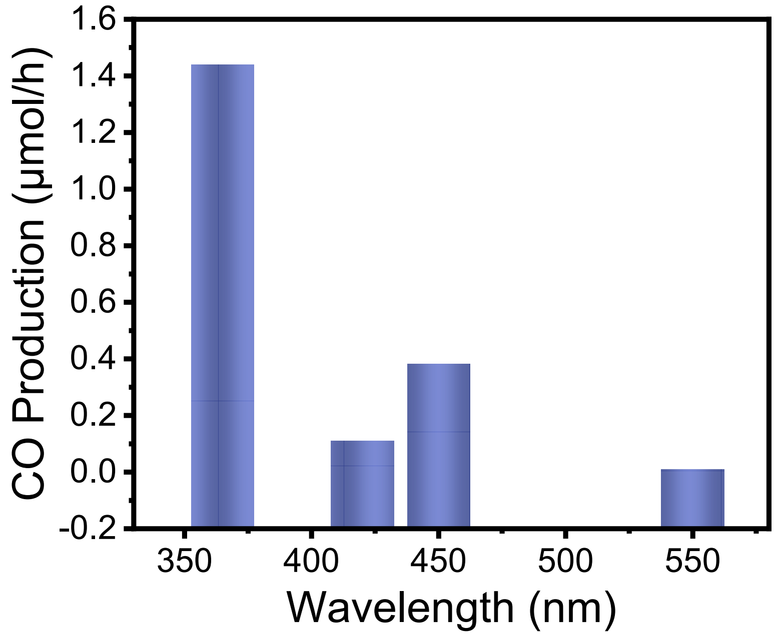

Figure S18. CO_2 photoreduction performance *vs*. wavelength.

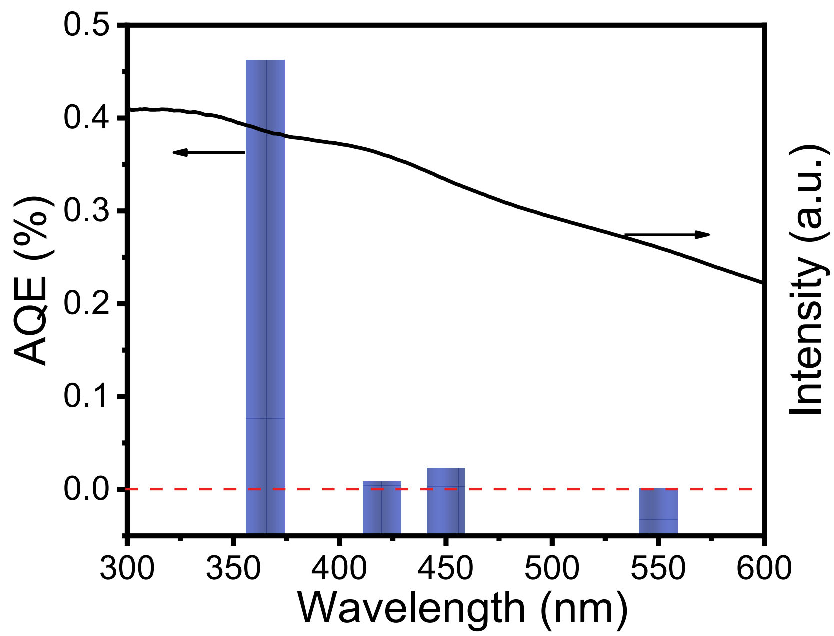

Figure S19. CO_2 photoreduction AQE *vs*. wavelength.

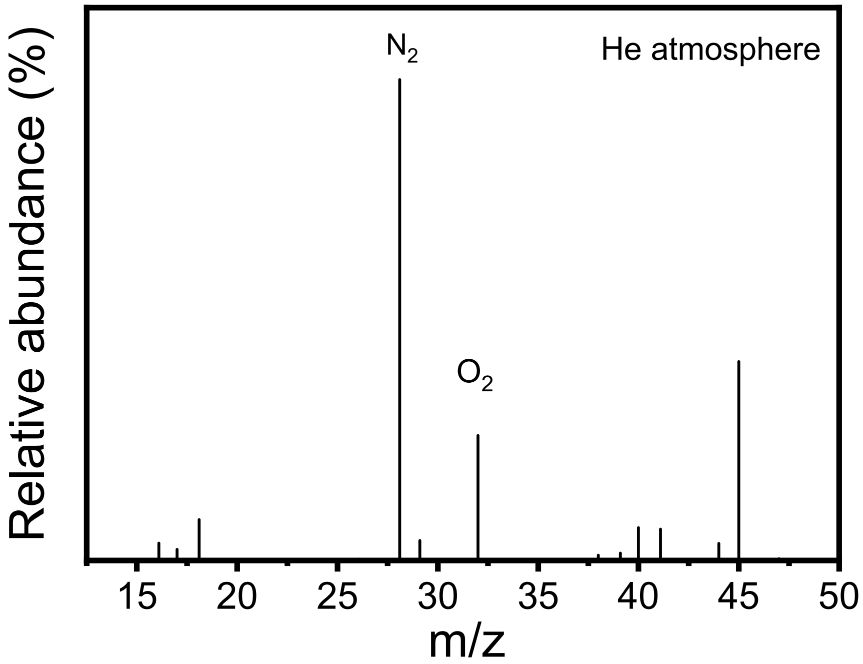

Figure S20. Mass spectra of headspace gas over Ru@Co-VOF in the photocatalytic system under He atomsphere.

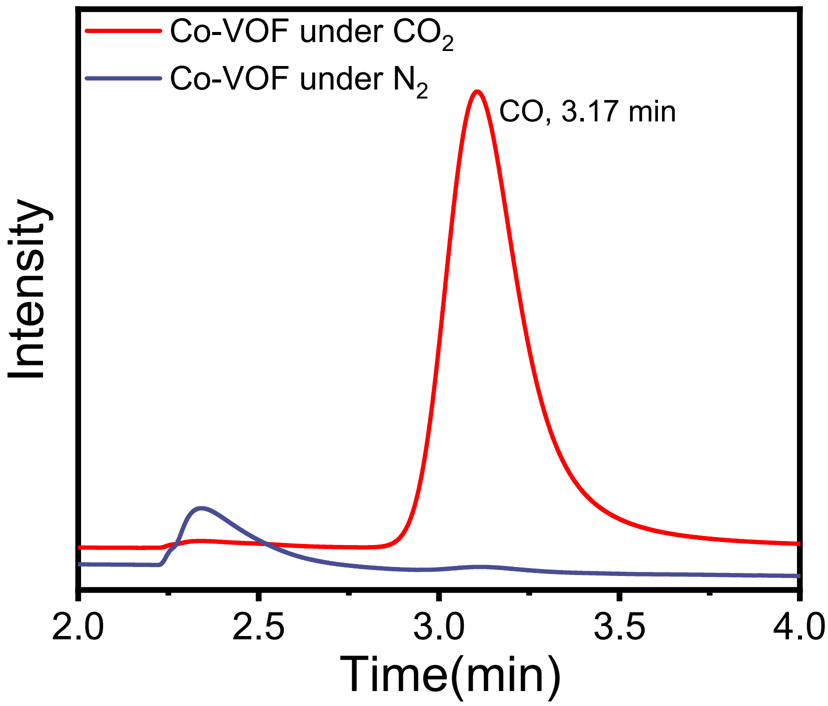

Figure S21. GC curve of CO over Ru@Co-VOF in the photocatalytic reduction under CO_2 and N_2 atomsphere.

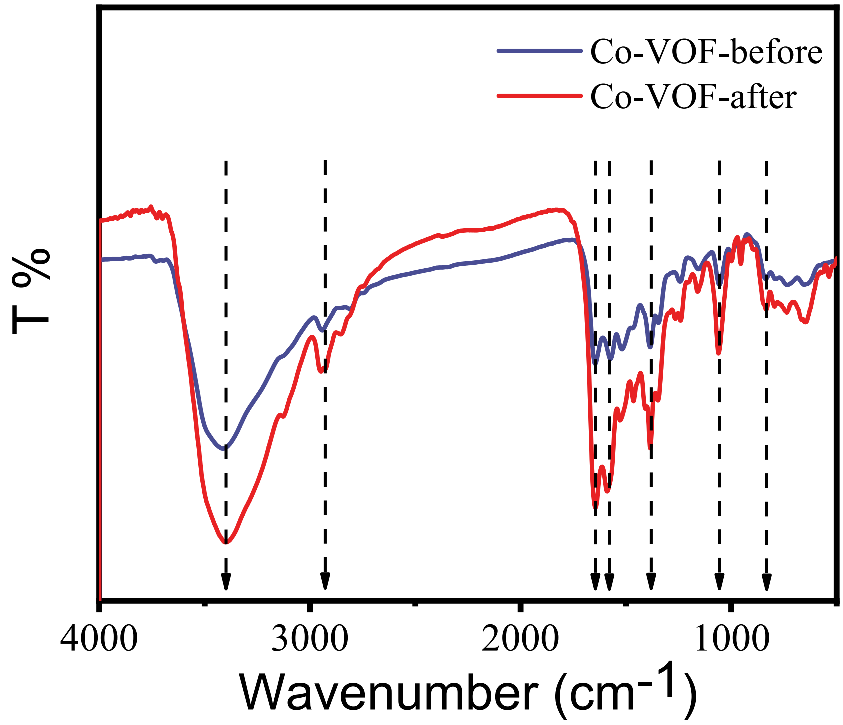

Figure S22. FT-IR spectra of Co-VOF before and after photocatalytic reaction.

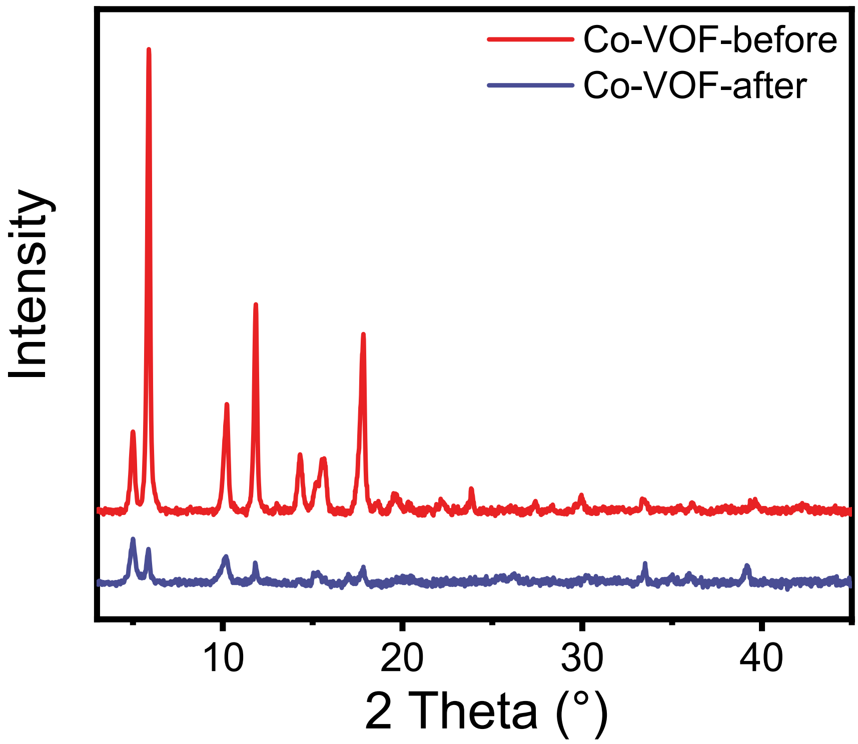

Figure S23. PXRD pattern of Co-VOF before and after photocatalytic reaction.

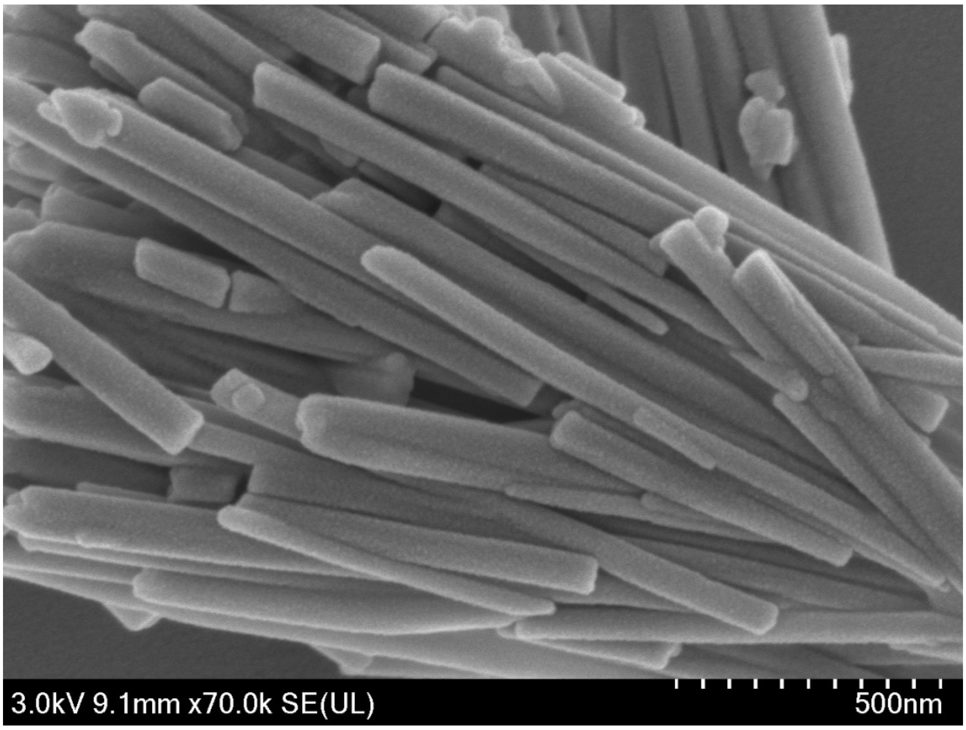

Figure S24. SEM image of Co-VOF after photocatalytic reaction.

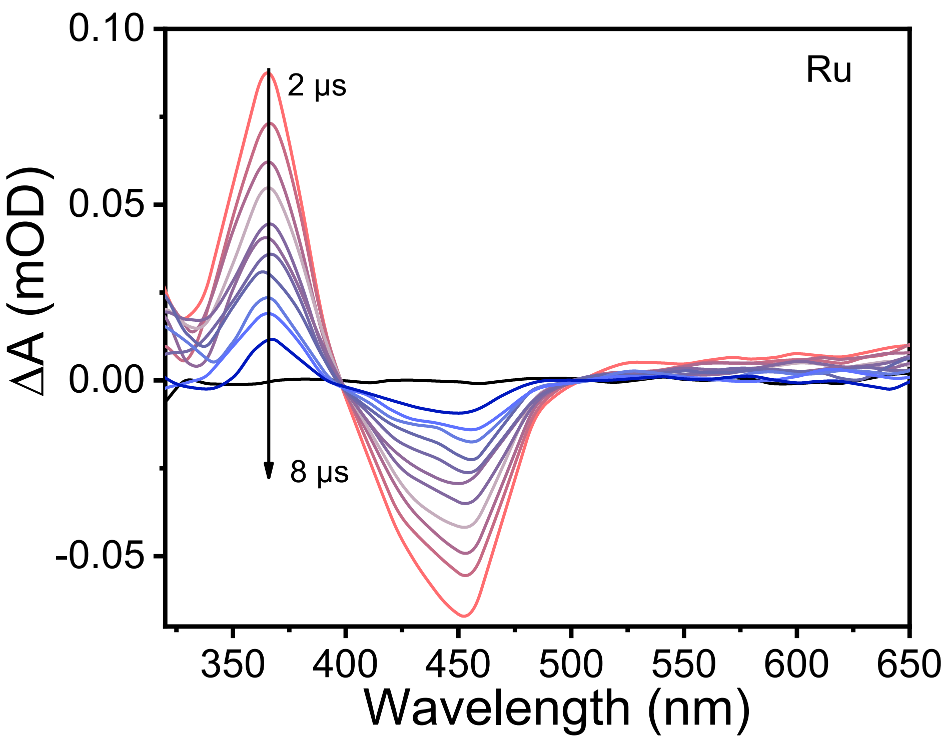

Figure S25. TA spectra of $Ru(bpy)_3^{2+}$ (50 μM).

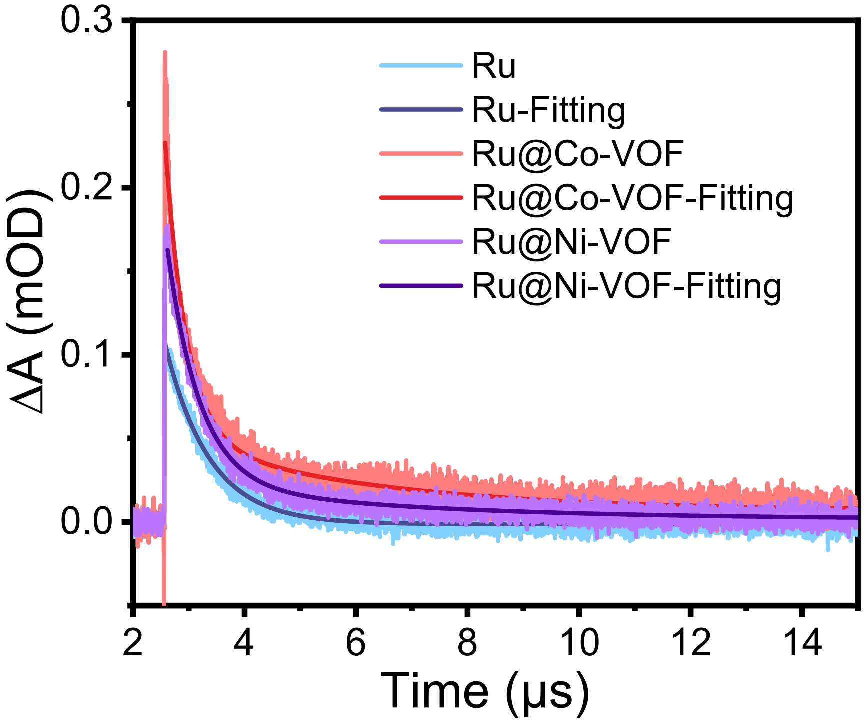

Figure S26. Kinetic traces of Ru, Ru @ Co-VOF, and Ru @ Ni-VOF at 370 nm. Conditions: λ_{ex} = 355 nm in CH_3CN under an Ar atmosphere.

Table S1. Some elements analysis of Ni-VOF and Co-VOF.

Simple	**N (%)**	**C (%)**	**H (%)**
Co-VOF	14.71	33.22	3.991
Ni-VOF	12.91	30.55	6.444

Table S2. Parameters for fitting the kinetic decay curve of the PL spectrum.

Sample	**Recovery Time (ns)**		**Average τ (ns)**
Ru	τ_1	70.1453	157.9874
	τ_2	160.1331	
Ru @ Ni-VOF	τ_1	2.66658	140.5678
	τ_2	158.1625	
Ru @ Co-VOF	τ_1	70.22946	157.9584
	τ_2	160.4134	

Table S3 Comparison of the performances of photocatalytic CO_2 conversion in similar systems.

catalyst	photosensitizer/ sacrificial agent	light source	irradiation time	catalyst dosage	reaction kinetic rate (μmol/h/g)	ref.
Co-VOF	$Ru(bpy)_3^{2+}$ TEOA	300W Xe ---	3h	5mg	CO 458.66	this work
Ni-MOF	$Ru(bpy)_3^{2+}$ TEOA	300W Xe ---	3h	5mg	CO 52.33	this work
$Co(P_4Mo_6)$	$Ru(bpy)_3^{2+}$ TEOA	300W Xe 400 nm< λ < 780 nm	10h	30mg	CO 1.07	1
MOF-808	$Ru(bpy)_3^{2+}$ H_2O	300W Xe 400 nm< λ < 800 nm	6h	3mg	CO 440	2
Re-Ru@MIL-101-NH_2(Al)	$Ru(bpy)_3^{2+}$ TEOA	5W LED λ=450 nm	10h	3.5mg	CO 19.19	3
$ZnFe_2O_4$/FeP-CTFs	$Ru(bpy)_3^{2+}$ TEOA	300W Xe λ≥420 nm	2h	5mg	CO 178	4
Ni COFs	$Ru(bpy)_3^{2+}$ TEOA	300W Xe λ≥420 nm	5h	10mg	CO 810	5
NH_2-MIL-101(Fe)	--- TEOA	300W Xe 400 nm< λ < 780 nm	5h	5mg	CO 17.52	6
$ZnMn_2O_4$	--- ---	500W Xe ---	8h	100mg	CO 26.2	7
BIF-101	$Ru(bpy)_3^{2+}$ TEOA	300W Xe λ≥400 nm	10h	10mg	CO 5830	8
Co(II)-MOF	$Ru(bpy)_3^{2+}$ BNAH	300W Xe λ≥400 nm	6h	4mg	CO 456	9
Co_1Ni_2-MOF	$Ru(phen)_3^{2+}$ TEOA	300W Xe λ≥420 nm	4h	2mg	CO 1160	10
Fe-MNS	$Ru(bpy)_3^{2+}$ TEOA	300W Xe λ≥420 nm	3h	5mg	CO 1637	11
Co/CTF-1	$Ru(bpy)_3^{2+}$ TEOA	300W Xe λ≥420 nm	4h	10mg	CO 50	12
Co-PMOF/GR	--- ---	300W Xe λ≥420 nm	8h	10mg	CO 20.25	13
Co-MOF-74	$Ru(bpy)_3^{2+}$ TEOA	300W Xe 400 nm< λ < 800 nm	2h	0.5 μmol	CO 2.01 μmol/h	14
Cu_2O@Cu@UiO-66-NH_2	--- TEOA	300W Xe λ>400 nm	5h	3mg	CO 20.9	15

References:

1. J. Du, Y. Ma, X. Xin, H. Na, Y. Zhao, H. Tan, Z. Han, Y. Li and Z. Kang, *Chemical Engineering Journal*, 2020, **398**, 125-518.

2. S. Karmakar, S. Barman, F. A. Rahimi and T. K. Maji, *Energy & Environmental Science*, 2021, **14**, 2429-2440.

3. P. M. Stanley, C. Thomas, E. Thyrhaug, A. Urstoeger, M. Schuster, J. Hauer, B. Rieger, J. Warnan and R. A. Fischer, *ACS Catalysis*, 2021, **11**, 871-882.

4. Y.-l. Yan, Q.-J. Fang, J.-k. Pan, J. Yang, L.-l. Zhang, W. Zhang, G.-l. Zhuang, X. Zhong, S.-w. Deng and J.-g. Wang, *Chemical Engineering Journal*, 2021, **408**,127-358.

5. W. Zhong, R. Sa, L. Li, Y. He, L. Li, J. Bi, Z. Zhuang, Y. Yu and Z. Zou, *J Am Chem Soc*, 2019, **141**, 7615-7621.

6. X. Y. Dao, J. H. Guo, Y. P. Wei, F. Guo, Y. Liu and W. Y. Sun, *Inorg Chem*, 2019, **58**, 8517-8524.

7. S. Yan, Y. Yu and Y. Cao, *Applied Surface Science*, 2019, **465**, 383-388.

8. Q.-L. Hong, H.-X. Zhang and J. Zhang, *Journal of Materials Chemistry A*, 2019, **7**, 17272-17276.

9. W.-M. Liao, J.-H. Zhang, Z. Wang, Y.-L. Lu, S.-Y. Yin, H.-P. Wang, Y.-N. Fan, M. Pan and C.-Y. Su, *Inorganic Chemistry*, 2018, **57**, 11436-11442.

10. J. Zhang, Y. Wang, H. Wang, D. Zhong and T. Lu, *Chinese Chemical Letters*, 2022, **33**, 2065-2068.

11. A. Mahmoud Idris, X. Jiang, J. Tan, Z. Cai, X. Lou, J. Wang and Z. Li, *J Colloid*

Interface Sci, 2022, **607**, 1180-1188.

12. J. Bi, B. Xu, L. Sun, H. Huang, S. Fang, L. Li and L. Wu, *Chempluschem*, 2019, **84**, 1149-1154.

13. L. Cheng, C. Wu, H. Feng and H. Liu, *Catalysis Science & Technology*, 2022, **12**, 7057-7064.

14. X. Deng, L. Yang, H. Huang, Y. Yang, S. Feng, M. Zeng, Q. Li and D. Xu, *Small*, 2019, **15**, 1902287.

15. S.-Q. Wang, X.-Y. Zhang, X.-Y. Dao, X.-M. Cheng and W.-Y. Sun, *ACS Applied Nano Materials*, 2020, **3**, 10437-10445.